Aerospace Science and Technology 15 (2011) 165–174

Contents lists available at ScienceDirect

Aerospace Science and Technology

www.elsevier.com/locate/aescte

# Evaluation of Recursive Least Squares algorithm for parameter estimation in aircraft real time applications

C. Kamali [a,*], A.A. Pashilkar [a], J.R. Raol [b]

[a] Flight Mechanics and Control Division, National Aerospace Laboratories, Bangalore-560017, India
[b] Dept. of E&C, MSRIT, Bangalore, India

ARTICLE INFO

*Article history:*
Received 8 September 2006
Received in revised form 11 December 2010
Accepted 17 December 2010
Available online 24 December 2010

*Keywords:*
Real-time parameter estimation
Fault tolerant control
Discrete Fourier transform
Recursive least squares
Stabilized RLS
Post failure model estimation
Calibrated air data
Stability margin

ABSTRACT

This paper presents results of evaluation of Recursive Least Squares (RLS) algorithm for real time applications in flight control and testing. The RLS proposed here is based on the equation error principle and can start with zero values of the unknown parameters. The technique makes use of only forgetting factor and a stabilizing parameter to achieve better convergence characteristics. In the present study, the RLS technique is applied for parameter estimation in the context of (i) reconfigurable/restructurable control, (ii) estimation of aircraft short period and Dutch roll characteristics in the absence of calibrated air data, and (iii) online stability (gain and phase) margin estimation.



## 1. Introduction

Parameter identification (PID) algorithms have potential application ranging from flight control, rapid flight envelope expansion, aerodynamic data update to the assessment of flight safety [12,3,5]. Online estimation algorithms are essential for reconfigurable/restructurable flight control. They are preferred in flight-testing to improve the efficiency of the testing process. There are many algorithms, which have been used for real-time parameter estimation. An evaluation of three recursive estimation algorithms was carried out in [1]. The work in [1] infers that the DFT technique proposed in [6] outperforms other techniques. Using the DFT technique, a simulation tool has been developed for on-line real time parameter estimation in [11]. The computational simplicity of equation error methods makes them more suitable for real time applications. In this paper, an evaluation of a time domain algorithm based on equation error RLS principle is carried out for: (i) application of on-line PID for post failure model estimation, (ii) developing a novel technique to perform on-line estimation of model parameters of a new aircraft undergoing developmental tests, assuming absence of calibrated air data, and (iii) developing a technique to evaluate real time stability margins, for an unstable aircraft. Hence, the motivation of present study is to show the suitability of one signal-processing tool (RLS), for three important problems. Nevertheless, there is an issue like numerical differentiation of noisy data [7] associated with this technique. This is successfully handled by using a digital filter in this paper.

Fault tolerant control systems within an aircraft have the potential of accommodating sensor and actuator failures. Simulation results presented in [8] have shown the potential of on-line DFT based PID within fault tolerant flight control system. Though the DFT technique performs well, it shows a relatively oscillatory/transient response until sufficient frequency domain information is obtained; its convergence rate is slow and requires higher floating point operations/cycle (hereafter we term it as FLOPS). The DFT technique is compared with a Bayesian method for the same application and the Bayesian technique outperforms DFT technique [2]. The Bayesian method is again iterative and computationally intensive. In this paper, we show that RLS in its stabilized version provides solution to the foregoing issues. The least squares algorithm with forgetting factor has tendency to become unstable under insufficiently excited conditions. A solution to this problem is proposed in [13] by including a stabilizing parameter and the resultant algorithm is called stabilized RLS (SRLS). The SRLS does not differ from RLS with respect to the asymptotic convergence properties because of the inclusion of stabilizing parameter (see Appendix A). A comparison of SRLS and DFT is carried out with respect to PID for reconfigurable/restructurable control. In RLS, requirement of noise covariance is compensated with forgetting fac-

* Corresponding author.
*E-mail addresses:* ckamali@css.nal.res.in (C. Kamali), apash@css.nal.res.in (A.A. Pashilkar), jrraol@yahoo.com (J.R. Raol).

1270-9638/$ – see front matter 
doi:10.1016/j.ast.2010.12.007

**Nomenclature**

| | | | |
|---|---|---|---|
| $\alpha$ | Angle of attack (AOA) | rad | |
| $p$ | Roll rate | rad/sec | |
| $r$ | Yaw rate | rad/sec | |
| $J$ | Cost function | | |
| $\delta_{el}$ | Left elevator deflection | rad | |
| $\delta a$ | Aileron deflection | rad | |
| $g$ | Acceleration due to gravity | m/sec$^2$ | |
| $\theta$ | Pitch angle | rad | |
| $\psi$ | Yaw angle | rad | |
| $N_{Y_{CG}}$ | Lateral acceleration at CG | | |
| $u$ *wind* | Forward wind velocity | ft/sec | |
| $w$ *wind* | Vertical wind velocity | ft/sec | |
| $\delta$ | Stabilizing parameter | | |
| $E$ | Expectation operator | | |
| $\beta$ | Angle of sideslip (AOSS) | rad | |
| $q$ | Pitch rate | rad/sec | |
| $\kappa$ | Vector of parameters (linear model) | | |
| $P$ | Covariance matrix | | |
| $\delta_{er}$ | Right elevator deflection | rad | |
| $\delta r$ | Rudder deflection | rad | |
| $V$ | True air speed | m/sec | |
| $\phi$ | Roll angle | rad | |
| $N_{Z_{CG}}$ | Normal acceleration at CG | | |
| $v$ *wind* | Lateral wind velocity | ft/sec | |
| $\lambda$ | Forgetting factor | | |
| $T$ | Denotes transposed variable | | |
| $\hat{}$ | Denotes an estimated variable | | |

*Acronyms*

| | |
|---|---|
| PID | Parameter identification |
| DFT | Discrete Fourier transform |
| 6 DOF | Six degrees of freedom |
| RLS | Recursive least squares |

tor. However, SRLS requires a stabilizing parameter in addition to the forgetting factor. The choice of forgetting factor and stabilizing factor does not affect the accuracy of final value of estimate in time. They only influence the convergence (faster and monotonic/less oscillatory) properties of the estimates with respect to time and hence the tuning is not very critical.

For a new aircraft undergoing developmental flight-tests, measurements of calibrated angle of attack ($\alpha$) and sideslip angle ($\beta$) will not be generally available. Under such circumstances, for the purpose of real time parameter estimation, Kalman filter (KF) and its variants can be used [12,3,5]. These algorithms are computationally complex and require proper process and measurement noise covariance for tuning the KF. RLS/SRLS does not need this and also avoids the need for direct angle of attack and sideslip measurements. Simulated data from six DOF non-linear flight simulation software are used to demonstrate this concept.

Many fighter aircraft are designed to be longitudinally unstable to gain good maneuverability. These aircraft are designed with highly augmented full authority control laws. When such aircraft undergo initial development flights, assessment of safety becomes very important. General method of assessing safety is by evaluating the phase and gain stability margins. Stability margins serve as a basis for the flight test ground support team to give clearance to the pilot to fly from one test point to the next. Flight clearance is given if the margins are satisfactory at the present test point. Most of the times, flight clearance analysis is performed off-line from the recorded flight-test data. Real time stability margin estimation is an attractive option to improve flight test efficiency. Technique achieving near real time estimation of stability margins using frequency response of aircraft data has been proposed in [10]. In place of frequency response model fitting, we apply the RLS algorithm to perform real time estimation of aircraft short period model for the purpose of stability margin computation to derive computational advantages. For the study of stability margin evaluation, measurements of angle of attack $\alpha$ and pitch rate $q$ are assumed to be available. If the angle of attack is not directly available, a combination of other signals including aircraft normal acceleration can be used to estimate the same. Similarly, the angle of sideslip is estimated using mainly the lateral acceleration signal.

The paper is organized as follows: Section 2 deals with application of on-line PID for nominal and post failure model estimation of faulty aircraft using SRLS and DFT. Section 3 describes the proposed methodology to perform on-line PID using RLS in absence of calibrated air data. Section 4 deals with the proposed scheme to evaluate real time stability margin using RLS. Section 5 summarizes the conclusions from this study.

## 2. Application of on-line PID for post failure estimation

On-line PID finds potential application in fault tolerant flight control systems. A fault tolerant flight control system is required to perform failure detection, identification and accommodation with the objectives 1) minimum handling quality degradation following a failure, 2) in the event of a failure, providing higher priority for the safe continuation of flight without aborting the mission, and 3) ensuring lower rate of aircraft loss. A block diagram of fault tolerant flight control system highlighting the role of on-line PID is shown in Fig. 1. A comparison of SRLS and DFT is carried out in this work. The algorithmic steps of DFT and RLS can be found in [4]. The steps in SRLS are:

Initialize the algorithm with

$$P(0) = (1/\delta)I \tag{1}$$

The covariance matrix is updated as follows:

$$\begin{aligned} P(n) = {} & \frac{1}{\lambda}P(n-1) \\ & - \frac{1}{\lambda}P(n-1)C(n) \\ & \times \left[\lambda I + C(n)^T P(n-1)C(n)\right]^{-1} C(n)^T P(n-1) \end{aligned} \tag{2}$$

where the matrix $C(n)$ is given by

$$C(n) = \begin{bmatrix} X^T(n) & \sqrt{n_p \delta(1-\lambda)}e(n) \end{bmatrix} \tag{3}$$

and $e(n)$ is a sequence of vectors

$$e(1) = \begin{bmatrix} 1 \\ 0 \\ \cdot \\ \cdot \\ \cdot \\ 0 \end{bmatrix}, \qquad e(2) = \begin{bmatrix} 0 \\ 1 \\ \cdot \\ \cdot \\ \cdot \\ 0 \end{bmatrix},$$

$$e(n_p) = \begin{bmatrix} 0 \\ 0 \\ \cdot \\ \cdot \\ \cdot \\ 1 \end{bmatrix}, \qquad e(n_p+1) = \begin{bmatrix} 1 \\ 0 \\ \cdot \\ \cdot \\ \cdot \\ 0 \end{bmatrix} \tag{4}$$

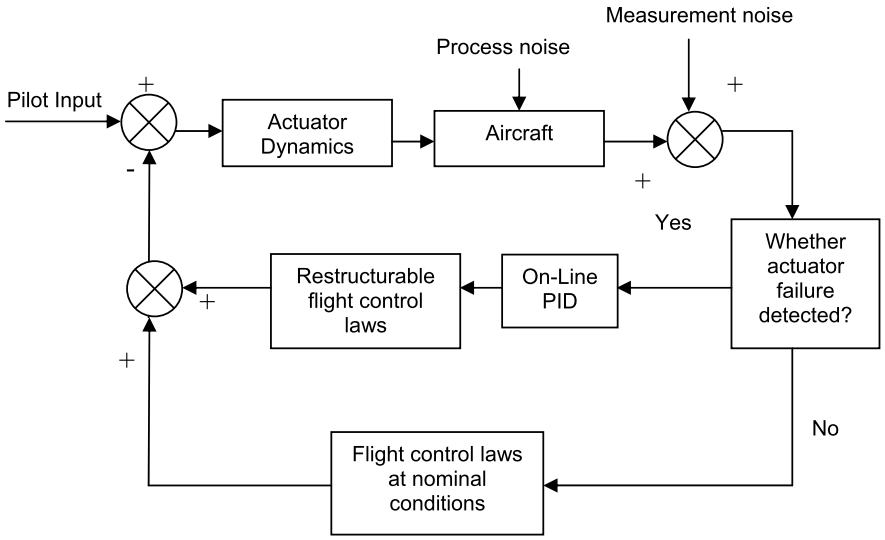


**Fig. 1.** A typical fault tolerant flight control system.

where $n_p$ is the number of parameters to be estimated in each of the state equation. The parameter update equation is given by:

$$\kappa(n) = \kappa(n-1) + P(n)X(n)^T\big[Y(n) - X(n)\kappa(n-1)\big] + \delta\lambda P(n)\big[\kappa(n-1) - \kappa(n-2)\big] \quad (5)$$

### 2.1. Post failure modeling

We assume actuator failure and/or battle damage. In general the elevator failure is considered to be more critical than aileron and rudder failures because of the unavoidable coupling between the longitudinal and lateral dynamics. Hence, this work considers only elevator failure. The aerodynamic characteristics of a control surface can be modeled in terms of normal force, axial force and moment around some fixed points or axes. We assume that the axial forces exerted by longitudinal control surface deflections are negligible and only the normal forces will undergo changes. Therefore, to derive a post failure model we need to obtain closed form expressions of the non-dimensional aerodynamic stability and control derivatives as function of the normal force coefficient relative to the control surface failure and/or battle damage [8]. In brief the closed-form expressions for the following derivatives in terms of $C_{L\delta}$ of left and right side of the longitudinal control surface are to be obtained: $C_{L\alpha}$, $C_{m\alpha}$, $C_{L\dot{\alpha}}$, $C_{m\dot{\alpha}}$, $C_{Lq}$, $C_{mq}$. A detailed study of post failure modeling of an aircraft involving a stuck left elevator with a 67% effectiveness reduction is covered in [8], from where the numerical values of nominal aircraft model and post failure model (Appendix B) are taken for the present simulation. It has been assumed that the left elevator gets stuck at 15 sec and also there is a loss of 67% in control surface effectiveness. It has also been assumed that the failure is detected in one second and the healthy right elevator is applied to perform PID.

### 2.2. Results and discussion — post failure model estimation

The PID was carried out featuring the nominal and post failure conditions in a single simulation process, considering clean and noisy simulated data. The PID implementation scheme reported here models left and right elevators separately for both the nominal conditions and post failure conditions. Comparison between RLS and DFT (with respect to FLOPS carried out in [4]) shows that RLS is superior to DFT in terms of minimum on-board memory. The LS algorithm with forgetting factor has a tendency to become

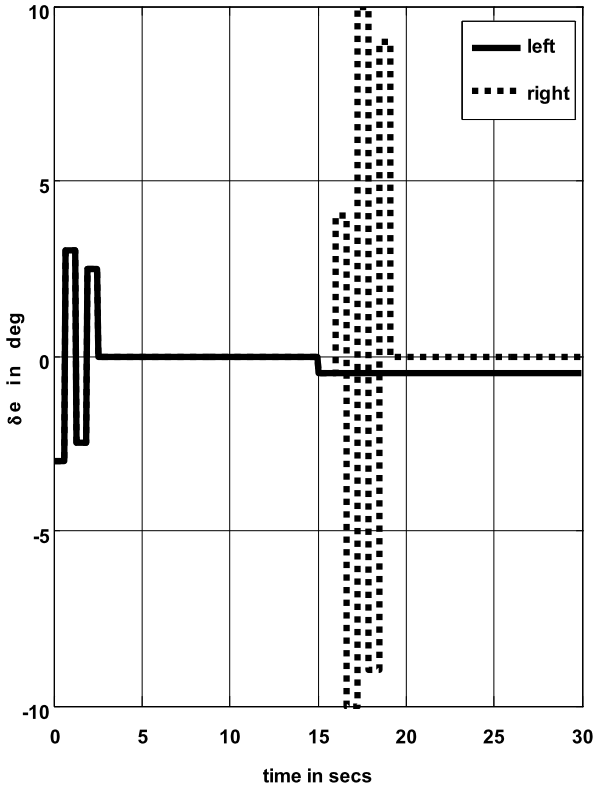


**Fig. 2.** Control surface inputs.

unstable under insufficiently excited conditions. One solution is to persistently excite the regression vector by adding a small perturbation to the controls by white noise. However, it will hamper the flight of the aircraft. Another solution is to use covariance resetting. This will induce sharp discontinuities and transients in the responses of the algorithm. The SRLS is a modified version of RLS, which avoids the need of covariance resetting during insufficiently excited conditions. The DFT technique does not require covariance resetting, as the entries of covariance matrix are nothing but recursive DFT update of state and control signals.

The control surface inputs showing the normal left and right elevators (0–15 sec) and normal right elevator with failed left ele-

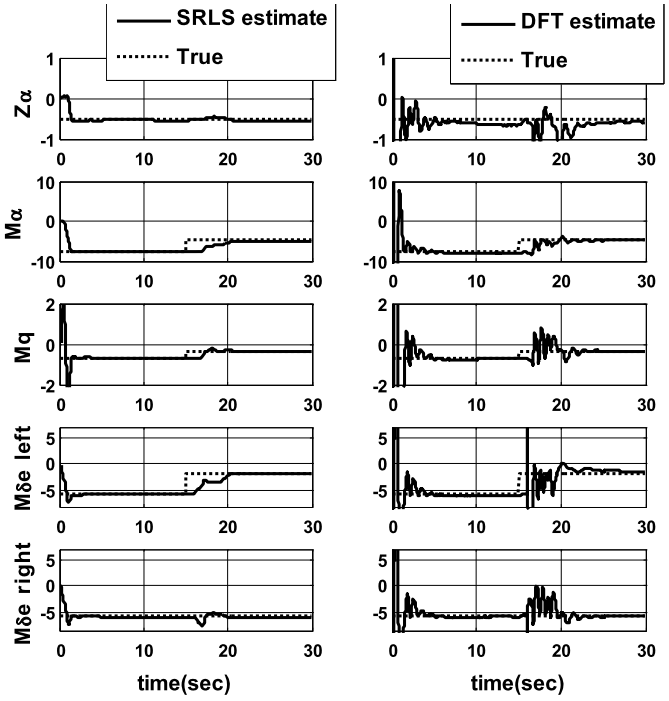


**Fig. 3.** Comparison of convergence between SRLS and DFT — noisy data (SNR = 10).

**Table 1**
Monte Carlo analysis for post failure model SRLS — noisy data (SNR = 10).

| Aircraft important short period parameters | True values under nominal conditions | Ensemble average of estimated values | True values under post failure conditions | Ensemble average of estimated values |
|---|---|---|---|---|
| $Z_\alpha$ | −0.5341 | −0.5341 | −0.5341 | −0.5313 |
| $M_\alpha$ | −7.7400 | −7.5591 | −4.7200 | −5.0346 |
| $M_q$ | −0.7173 | −0.6764 | −0.3800 | −0.4032 |
| $M_{\delta e\text{-left}}$ | −5.7000 | −5.5889 | −1.8990 | −1.9480 |
| $M_{\delta e\text{-right}}$ | −5.7000 | −5.5889 | −5.7000 | −5.9724 |
| PEEN | 2.1683 | | 5.4727 | |

vator (15–30 sec) are shown in Fig. 2. The aircraft responses $(\alpha, q)$ are corrupted by Gaussian measurement noise with SNR = 10. The convergence of parameters along with their true values for SRLS and DFT schemes are plotted in Fig. 3. The convergence of SRLS is found to be less oscillatory, monotonic and faster than DFT. The smoother convergence of SRLS is because of the use of stabilizing parameter $\delta$ that penalizes the estimates deviating from their previous values. The regularizing parameter $\delta$ was chosen to be 10. The use of $\delta$ is equivalent to introducing damping effect in convergence characteristics. Larger the value of $\delta$, slower will be the convergence. However, the choice of $\delta$ does not hamper the estimation accuracy. The forgetting factor $\lambda$ is chosen to be 0.999. A Monte Carlo simulation of 500 runs was performed for SRLS with noisy data (SNR = 10). The result of Monte Carlo simulation is presented in Table 1. The estimated results are satisfactory. In tables PEEN represents Parameter Estimation Error Norm calculated as:

$$\text{PEEN} = \frac{norm(\kappa_t - \hat{\kappa})}{norm(\kappa_t)} \times 100 \tag{6}$$

Here, $\kappa_t$ is the vector of true parameters and $\hat{\kappa}$ is the vector of estimated parameters.

## 3. Estimation in absence of calibrated angles of incidence and sideslip

Basically the RLS proposed here assumes the measurement of $\alpha$ for estimation of aircraft short period data and $\beta$ for estimation of Dutch roll data. When the calibrated measurements of $\alpha$ and $\beta$ are not available, they can be reconstructed on-line using normal acceleration ($N_{z_{CG}}$) and lateral acceleration ($N_{y_{CG}}$) measured at center of gravity (CG) of aircraft respectively. Typically, the onboard inertial platform senses the local acceleration, which is a combination of acceleration at CG as well as the angular rates. The acceleration variables are measured at sensor location, which has a definite relation with acceleration at CG. For example

$$N_{z_{sensor}} = N_{z_{CG}} + \dot{q}x_s \tag{7}$$

where $x_s$ is the forward displacement (in meters) of the accelerometer sensor from the CG in the $x$ direction. If the measurement of $N_{z_{CG}}$ is not available then using $N_{z_{sensor}}$ and filtered differentiation of pitch rate one can obtain $N_{z_{CG}}$. Similar conclusion applies to $N_{y_{CG}}$.

### 3.1. Development of mathematical models

The AOA and AOSS can be constructed on-line by mathematically integrating the following equations:

$$\dot{\alpha} = q + \frac{g}{V}(\cos\theta\cos\phi + N_{z_{CG}}),$$
$$\dot{\beta} = p\sin\alpha_0 - r\cos\alpha_0 + \frac{g}{V}(N_{y_{CG}} + \sin\phi) \tag{8}$$

where $\alpha_0$ is the trim value of angle of attack. Eq. (8) has been derived by us from the basic flight mechanics equations found in [9]. The reconstructed values of $\alpha$ and $\beta$ can be utilized by the proposed algorithm to yield real time parameter estimates. Block diagrams showing the methodology of conducting on-line PID in absence of calibrated air data are shown in Fig. 4. The acceleration related variables $N_{z_{CG}}$ and $N_{y_{CG}}$ are noisy and integration of those variables will introduce drift in the derived $\alpha$ and $\beta$. The unwanted drift in derived $\alpha$ and $\beta$ affects estimation accuracy. Hence, in this paper, we propose a solution to this problem. The aircraft state space model to be estimated can include a constant term for modeling the drift. The short period model to be estimated can be augmented with drift constants $k_1$ and $k_2$ as follows:

$$\begin{bmatrix}\dot{\alpha}\\ \dot{q}\end{bmatrix} = \begin{bmatrix}Z_\alpha & Z_q\\ M_\alpha & M_q\end{bmatrix}\begin{bmatrix}\alpha\\ q\end{bmatrix} + \begin{bmatrix}Z_{\delta e} & k_1\\ M_{\delta e} & k_2\end{bmatrix}\begin{bmatrix}\delta_{el}\\ u_s\end{bmatrix} \tag{9}$$

Similarly the second order Dutch roll lateral model can be augmented with drift constants $k_1$ and $k_2$ as follows:

$$\begin{bmatrix}\dot{p}\\ \dot{r}\end{bmatrix} = \begin{bmatrix}L_p & L_r\\ N_p & N_r\end{bmatrix}\begin{bmatrix}p\\ r\end{bmatrix} + \begin{bmatrix}L_\beta & L_{\delta a} & L_{\delta r} & k_1\\ N_\beta & N_{\delta a} & N_{\delta r} & k_2\end{bmatrix}\begin{bmatrix}\beta\\ \delta a\\ \delta r\\ u_s\end{bmatrix} \tag{10}$$

Here, $u_s$ represents discrete unit step signal. Modeling the aircraft dynamics with augmented drift constants and then estimating the parameters using RLS algorithm will yield the best LS solution while using derived $\alpha$ and $\beta$ from the noisy acceleration signals.

### 3.2. Results and discussion — short period

The data required for the short period real time parameter estimation have been generated using 6 DOF flight simulation software. This software models the dynamics of an unstable/highly augmented fighter aircraft. Initially, data for a subsonic flight condition were generated. This represents the landing phase of aircraft

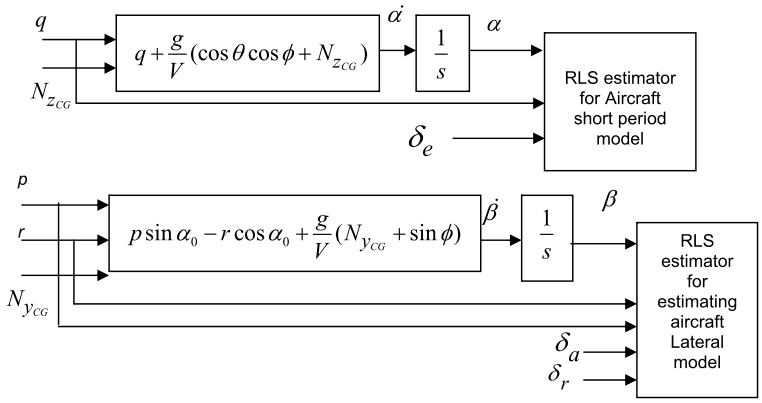


**Fig. 4.** Block diagram of estimation scheme in absence of calibrated air data.

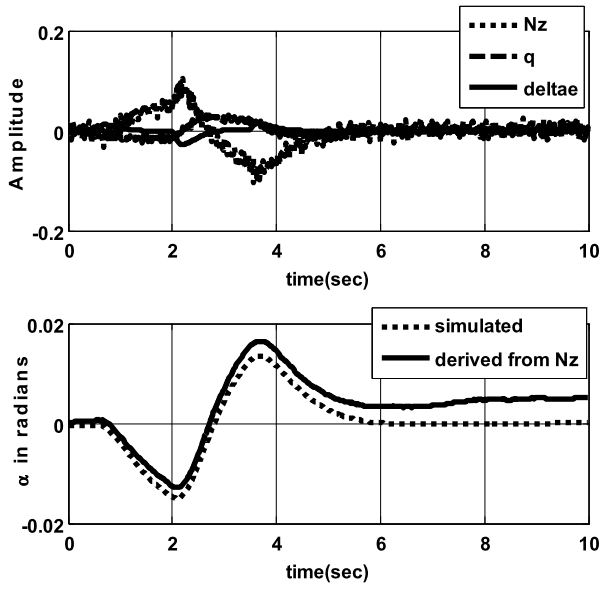


**Fig. 5.** Match of constructed alpha with simulated alpha.

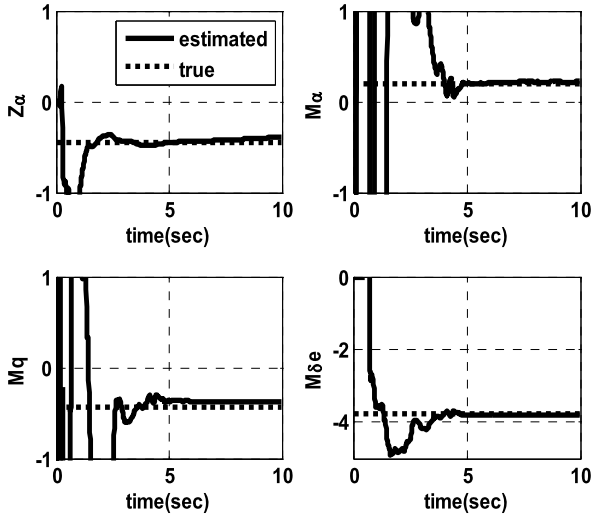


**Fig. 6.** Convergence of important short period parameters — noisy data.

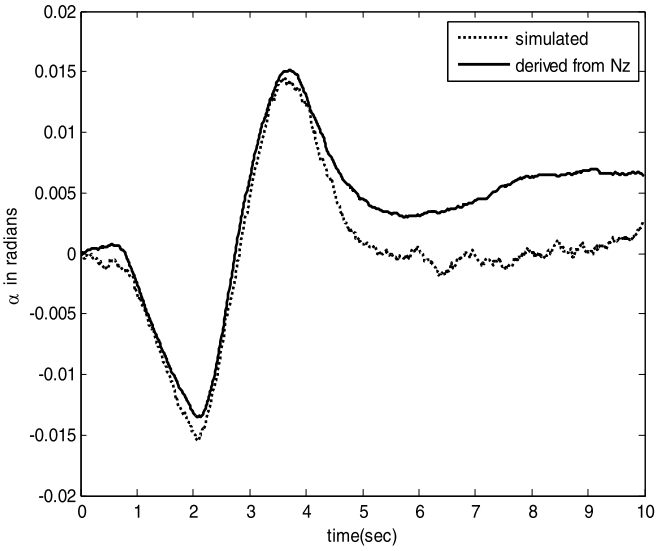


**Fig. 7.** Match of constructed alpha with simulated alpha — under turbulence.

and the aircraft short period model is unstable for this flight condition. The convergence was satisfactory. In order to test the robustness of algorithm to measurement noise, the estimation was repeated with responses $(\alpha, q)$ corrupted by Gaussian random noise with SNR = 10. The noisy $N_{z_{CG}}$ and $q$ signals are shown in Fig. 5. $\delta_e$ is assumed uncorrupted by measurement noise. The comparison of constructed $\alpha$ with simulated $\alpha$ is shown in Fig. 5. The constructed $\alpha$ shows a drift. This drift is taken care in the modeling so that we could still get reasonably good estimates. The convergence plots for important short period parameters are shown in Fig. 6. Subsequently, the algorithm was tested for a transonic and supersonic simulated data with and without measurement noise. The supersonic data was corrupted with Gaussian noise with SNR = 100, since $\delta_e$ and $\alpha$ amplitudes were significantly low at supersonic flight conditions. The estimated results for noisy flight data are presented in Table 2. The quantified assessment of estimates in Table 2 is computed using PEEN. The estimated parameters are satisfactory. If the augmentation proposed for drift terms in Eq. (9) is not applied, the parameter estimates are found to deviate significantly from the true values.

### 3.2.1. Performance under turbulent conditions

The equation error RLS/SRLS discussed in this paper is not modified to perform under turbulent wind conditions. However, a mild turbulence profile of intensity 0.5 ft/sec in the forward velocity and vertical velocity is invoked in the simulation apart from sensor measurement noise to evaluate longitudinal estimation performance. The reconstructed $\alpha$ is shown in Fig. 7 that diverges beyond 5 sec. Despite accounting for drift through a constant in estimation, it can be noticed that the $z_\alpha$ shows some tendency to

**Table 2**
Short period model estimation in absence of calibrated alpha — noisy data.

| Aircraft short period parameters | Subsonic flight condition Noisy data, SNR = 10 | | Transonic flight condition Noisy data, SNR = 10 | | Supersonic flight condition Noisy data, SNR = 100 | |
|---|---|---|---|---|---|---|
| | True values | RLS estimates | True values | RLS estimates | True values | RLS estimates |
| $Z_\alpha$ | −0.4445 | −0.3888 | −0.8420 | −0.7849 | −1.0601 | −1.0099 |
| $Z_q$ | 0.9723 | 0.9213 | 0.9866 | 0.9699 | 0.9897 | 0.9891 |
| $Z_{\delta e}$ | −0.1812 | −0.2285 | −0.3305 | −0.2867 | −0.1987 | −0.1262 |
| $M_\alpha$ | 0.1985 | 0.2260 | −4.9170 | −4.6882 | −25.0863 | −23.2986 |
| $M_q$ | −0.4276 | −0.3759 | −1.6163 | −1.7011 | −0.7066 | −0.6623 |
| $M_{\delta e}$ | −3.7559 | −3.8148 | −34.9966 | −34.9109 | −31.6478 | −30.0560 |
| PEEN | 2.5308 | | 0.7580 | | 5.9299 | |

**Table 3**
Dutch roll model estimation in absence of calibrated beta — noisy data (SNR = 10).

| Aircraft lateral Dutch roll parameters | Subsonic flight condition Noisy data, SNR = 10 | | Transonic flight condition Noisy data, SNR = 10 | | Supersonic flight condition Noisy data, SNR = 10 | |
|---|---|---|---|---|---|---|
| | True values | RLS estimates | True values | RLS estimates | True values | RLS estimates |
| $L_p$ | −0.8225 | −0.7428 | −1.9243 | −1.8073 | −2.2303 | −2.0555 |
| $L_r$ | 0.7550 | 0.7872 | 1.6293 | 1.3635 | 0.7982 | 0.5494 |
| $L_\beta$ | −10.5247 | −10.0654 | −34.1738 | −34.5821 | −68.5839 | −67.5606 |
| $L_{\delta a}$ | −17.5596 | −17.0116 | −103.9980 | −102.1150 | −102.7930 | −99.7406 |
| $L_{\delta r}$ | 1.7896 | 1.8133 | 12.2560 | 13.3267 | 6.1486 | 7.2836 |
| $N_p$ | −0.0407 | −0.0671 | −0.0668 | −0.0362 | −0.0708 | −0.0790 |
| $N_r$ | −0.1372 | −0.1545 | −0.3441 | −0.3779 | −0.3986 | −0.3722 |
| $N_\beta$ | 1.6028 | 1.5515 | 9.2116 | 9.5582 | 13.7021 | 12.7345 |
| $N_{\delta a}$ | −1.3991 | −1.2770 | −10.7622 | −10.0055 | −14.5241 | −14.1312 |
| $N_{\delta r}$ | −1.0054 | −1.0789 | −5.2965 | −4.9197 | −3.5646 | −3.2622 |
| PEEN | 3.5110 | | 2.1351 | | 2.7710 | |

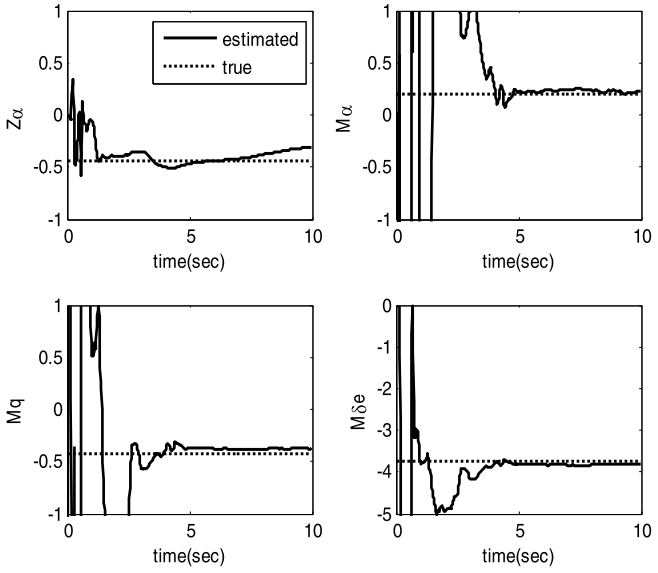


**Fig. 8.** Convergence of important short period parameters — under turbulence.

diverge in Fig. 8 compared to Fig. 6. Nevertheless, for this wind profile the PEEN value is found to be 5.177 which is satisfactory.

### 3.3. Results and discussion — Dutch roll

The required data for Dutch roll were simulated for the same aircraft. As before, we tested the estimator with a simulated data set representing subsonic flight condition. The convergence was satisfactory. To test the robustness of the technique, the subsonic data were corrupted by Gaussian measurement noise with SNR = 10. The noisy time histories are shown in Fig. 9. The reconstructed $\beta$ is found to match with simulated beta in Fig. 9. The convergence of important lateral Dutch roll parameters is seen in Fig. 10. The convergence is satisfactory. The algorithm was tested for a transonic and supersonic simulated data with and without measurement noise. The estimated results for noisy flight data are presented in Table 3. The estimates are assessed in Table 3 using PEEN. The RLS algorithm performs satisfactorily. If the augmentation proposed for drift terms in Eq. (10) is not applied, the parameter estimates are found to deviate significantly from the true values.

#### 3.3.1. Performance under turbulent conditions

A mild turbulence profile of intensity 0.5 ft/sec in the side velocity is invoked in the simulation apart from sensor measurement noise to evaluate lateral estimation performance. The reconstructed $\beta$ is shown in Fig. 11 that deviates beyond 4 sec. Despite accounting for drift through a constant in estimation, it can be noticed that the $L_p$, $L_\beta$, $N_\beta$, $L_{\delta a}$ deviate from the true values significantly as shown in Fig. 12 compared to Fig. 10. This increases the PEEN to 36.6414, which is not satisfactory. Further study is required in this direction to improve the results. May be the model of turbulence along with the measurement noise covariance matrix $R$ should be incorporated in the RLS scheme.

## 4. Proposed methodology for real time stability margin estimation

The block diagram showing phases involved in the proposed methodology to perform real time stability margin estimation is given in Fig. 13. Phase (i) incorporates a real time parameter estimation algorithm for estimating aircraft short period model. In phase (ii) the product of estimated short period model and (controller + actuator) transfer function (TF) is computed to yield loop transfer function. It should be noted that phase (ii) can be made real time by pre-computing the controller + actuator TF.

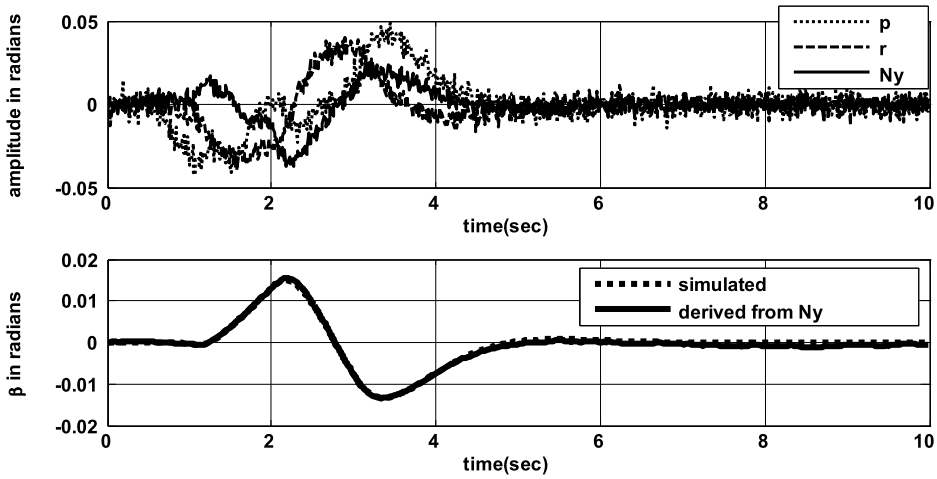


**Fig. 9.** Match of constructed beta with simulated beta — noisy data.

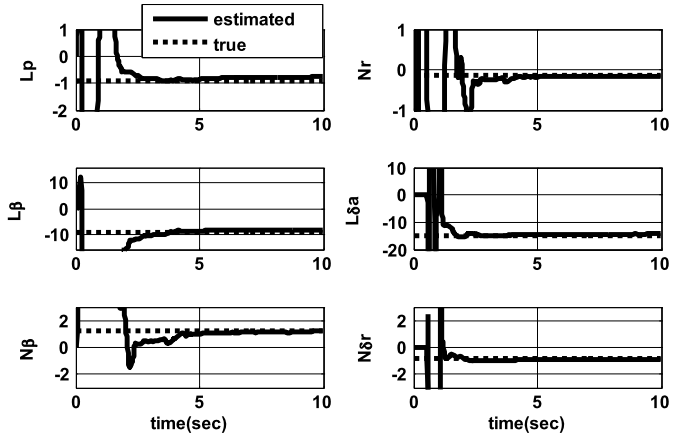


**Fig. 10.** Convergence of important Dutch roll parameters to true values — noisy data.

From the open loop TF phase margin and gain margin values are evaluated.

### 4.1. Description of unstable aircraft model — stability margin estimation

The basic aircraft model chosen for this exercise is longitudinally unstable. The mathematical model of the unstable aircraft is given in Eq. (11). The longitudinal dynamics of aircraft has two modes namely short period mode and phugoid mode. The left top corner of $A$ matrix and top two elements of $B$ matrix shown in the partitions of Eq. (11) represent the aircraft short period parameters. Similarly the right bottom corner of $A$ matrix and bottom two elements of $B$ matrix shown in the partitions of Eq. (11) represent the aircraft phugoid parameters. There is a certain amount of coupling between the short period and the phugoid characteristics.

$$\begin{bmatrix} \dot{\alpha} \\ \dot{q} \\ \dot{\theta} \\ \dot{u}/u_0 \end{bmatrix} = \left[\begin{array}{cc|cc} Z_\alpha & 1 & 0 & Z_{\dot{u}/u_0} \\ M_\alpha & M_q & 0 & M_{\dot{u}/u_0} \\ \hline 0 & 1 & 0 & 0 \\ X_\alpha & 0 & X_\theta & X_{\dot{u}/u_0} \end{array}\right] \begin{bmatrix} \alpha \\ q \\ \theta \\ u/u_0 \end{bmatrix} + \left[\begin{array}{c} Z_{\delta e} \\ M_{\delta e} \\ \hline 0 \\ X_{\delta e} \end{array}\right] \delta_e \tag{11}$$

The numerical values of above state model can be found in Appendix C. The instability for this longitudinal model is mainly caused by the short period dynamics. Therefore, we estimate only the short period parameters for the purpose of computing stability margin.

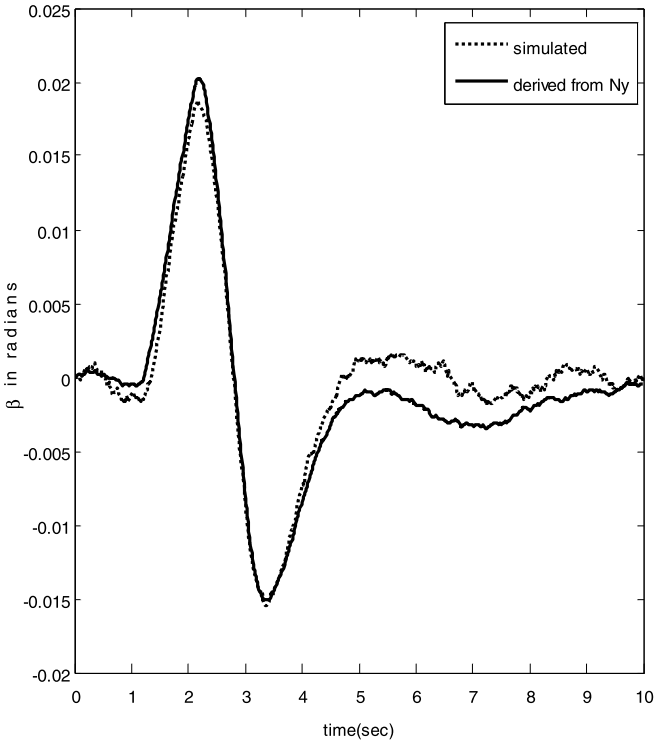


**Fig. 11.** Match of constructed beta with simulated beta — under turbulence.

### 4.2. Results and discussion of stability margin

Initially, to demonstrate the concept of stability margin estimation, the simulated closed loop responses $(\alpha, q)$ of the aircraft are assumed to be free from measurement noise. It was observed that the on-line estimated short period parameters converged as soon as the maneuver was over. This facilitated the computation of stability margins around 3.5 seconds itself. However results are calculated for data up to the end of 10-second simulation. The estimated stability margin values along with the true values are given in Table 4. The accuracy of estimates in Table 4 is quantified as per the criteria reported in [10]. In order to test the robustness of RLS estimator to noisy data, Gaussian measurement noise with

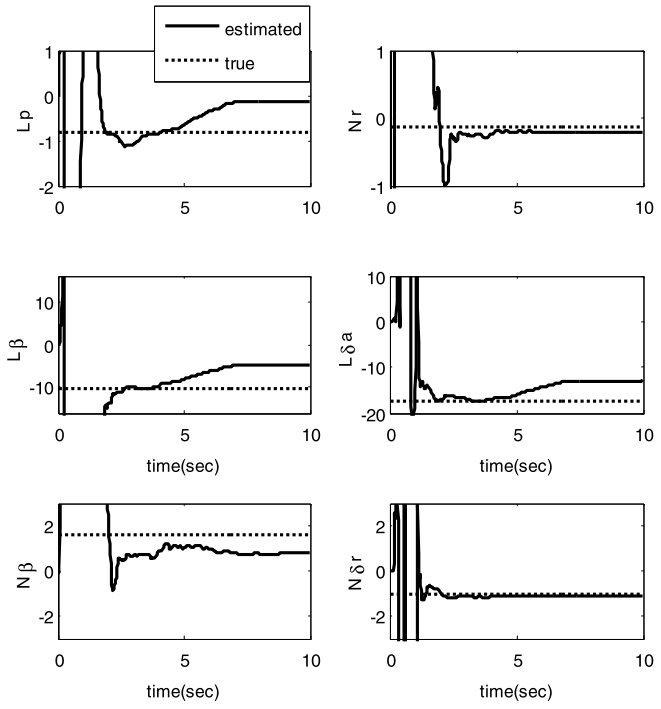


**Fig. 12.** Convergence of important Dutch roll parameters — under turbulence.

SNR = 10 was added to the closed responses $\alpha$ and $q$. The control surface input is assumed to be free from measurement noise. Even with noisy data the estimated parameters converged as soon as the maneuver was over. Bode plots are shown in Fig. 14 for the true open loop transfer function and estimated loop transfer function. The matching between the Bode plots looks very satisfactory for noisy data. The estimated stability margin values obtained with noisy data along with the true values are given in Table 4.

## 5. Conclusions

This paper presents practical applications of RLS algorithm in flight control and testing. Based on the study the following conclusions are drawn:

An evaluation for post failure aircraft model estimation using SRLS and DFT techniques shows the superiority of SRLS over DFT in terms of transient, convergence characteristics and FLOPS**,** which are the important requirements in adaptive control. The asymptotic convergence of SRLS has been derived in Appendix A.

A novel technique for real time parameter estimation using RLS in absence of calibrated angle of attack and sideslip is proposed. The technique is demonstrated to work with reconstructed alpha and beta from normal and lateral accelerations respectively. We have also shown that the drift found in the reconstructed alpha and beta due to noisy data assumptions can be suitably accounted in aircraft state space model, so that it does not affect the estimation accuracy. The concept is validated using realistic simulated data covering subsonic, transonic and supersonic flight conditions for the aircraft short period and Dutch roll dynamics. However, the performance under turbulent conditions is not satisfactory. Hence,

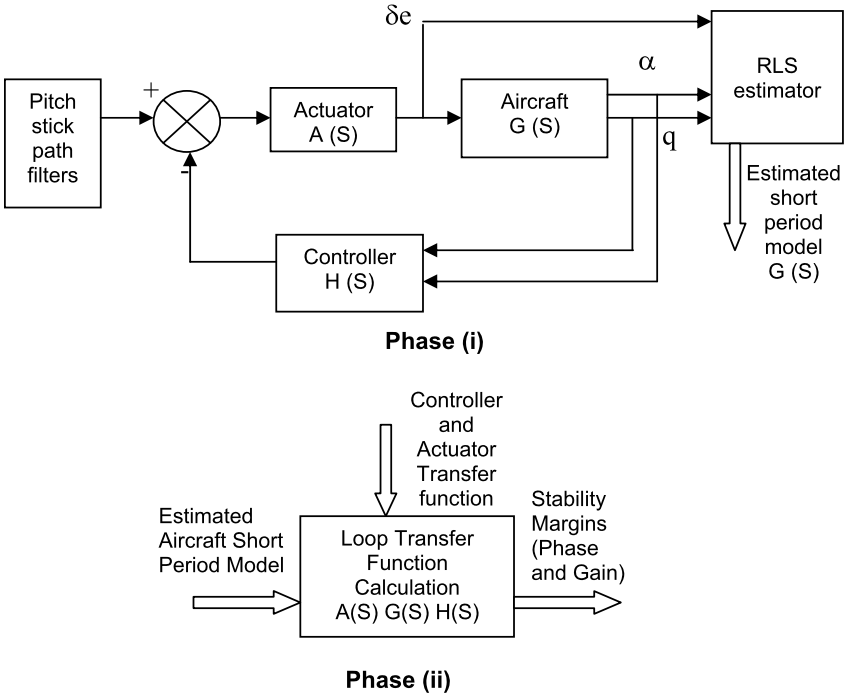


**Fig. 13.** Phases involved in the proposed scheme of real time stability margin estimation.

**Table 4**
Estimated values of stability margin.

| Cases | Estimated valued | | True values | | Error (True − Estimated) | |
|---|---|---|---|---|---|---|
| | Phase margin (deg) | Gain margin (dB) | Phase margin (deg) | Gain margin (dB) | Phase margin (deg) | Gain margin (dB) |
| Clean data | 58.1996 | Infinity | 57.9339 | Infinity | −0.2657 | 0 |
| Noisy data, SNR = 10 | 57.9805 | Infinity | 57.9339 | Infinity | −0.0466 | 0 |

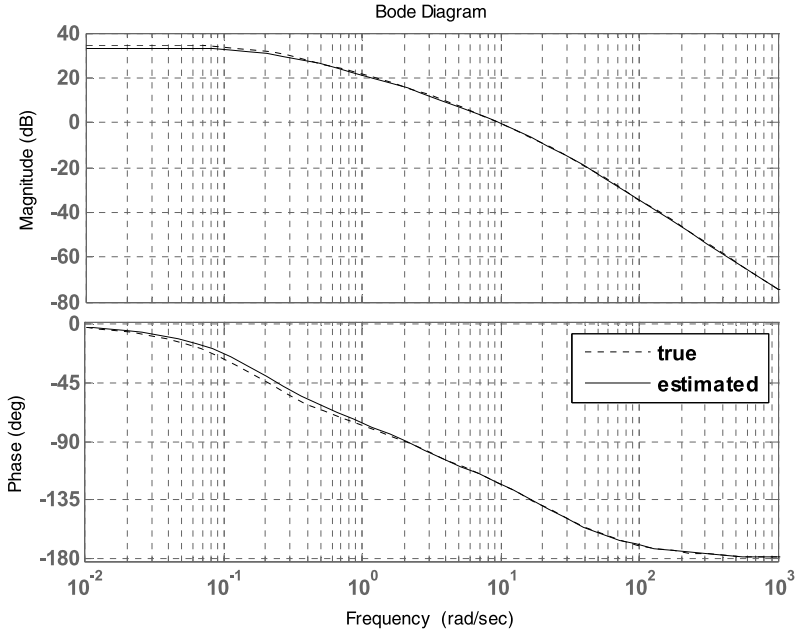


**Fig. 14.** Bode plots for the true model and estimated model — noisy data (SNR = 10).

this leaves a future scope to account wind (model) along with the measurement covariance matrix into the estimation to improve the accuracy.

A novel application of RLS to real time aircraft stability margin evaluation has been demonstrated. The proposed scheme is found to be robust for data corrupted with Gaussian measurement noise of SNR = 10.

Finally, it should be mentioned that the above schemes could be easily flight tested to evaluate the suitability of RLS on-board for the three important problems discussed in this paper.

## Acknowledgements

The technical discussions with Dr. Jatinder Singh, Scientist, FMCD, NAL, during this work are gratefully acknowledged. We sincerely thank the reviewers for their valuable comments.

## Appendix A. Asymptotic convergence of SRLS estimator to true value

The cost function of stabilized RLS is as follows:

$$J\big(\kappa(N)\big) = \sum_{k=1}^{N} \big|Y(k) - \kappa^T(N)X(k)\big|^2 \lambda^{N-k} + \delta\big|\kappa(N) - \kappa(N-1)\big|^2 \tag{12}$$

Setting $\partial J(\kappa(N))/\partial\kappa(N) = 0$, yields the optimal estimate of $\kappa(N)$.

$$\hat{\kappa}(N) = \left[\sum_{k=1}^{N} X^T(k)X(k)\lambda^{N-k} + \delta I\right]^{-1} \times \left[\sum_{k=1}^{N} X^T(k)Y(k)\lambda^{N-k} + \delta\kappa(N-1)\right] \tag{13}$$

In this study we make use of this solution to show the asymptotic convergence of estimator to its true value, as SRLS is nothing but the recursive form of Eq. (13).

The information matrix is defined as:

$$\phi(N) = \sum_{k=1}^{N} \lambda^{N-k} X^T(k)X(k) + \delta I \tag{14}$$

The inverse of information matrix is covariance matrix $P(N)$. We write the linear regression model at the $N$th time instant as:

$$Y(N) = X^T(N)\kappa + \varepsilon(N) \tag{15}$$

where $\varepsilon$ is the measurement error process which is assumed to be white with zero mean and variance $\sigma^2$ and $\kappa$ is the true value. Now substituting Eq. (15) in Eq. (13), also assuming $\lambda = 1$ for the sake of computational simplicity and rearranging the equation yields

$$\hat{\kappa}(N) = \phi^{-1}(N)\big(\big(\phi(N) - \delta I\big)\kappa\big) + \phi^{-1}(N)\left(\sum_{k=1}^{N} X^T(k)\varepsilon(k)\right) + \big(\phi^{-1}(N)\delta\hat{\kappa}(N-1)\big) \tag{16}$$

Taking the expectation operator on both sides of Eq. (16), and knowing from the principle of orthogonality that all elements of the tap input vector $X(k)$ are orthogonal to the measurement error process $\varepsilon(k)$, and rearranging, Eq. (16) yields

$$E\big[\hat{\kappa}(N)\big] = \kappa - \delta\phi^{-1}(N)\kappa + \phi^{-1}(N)\delta E\big(\hat{\kappa}(N-1)\big) \tag{17}$$

We write the expression for bias in the estimator as

$$b(N) = E\big[\hat{\kappa}(N)\big] - \kappa \tag{18}$$

Let $R$ denote the $M$ by $M$ ensemble averaged information matrix of vector $X(N)$. Assuming that the random process $X(N)$ is ergodic, it is well known that for large $N$, we may approximate write:

$$\frac{R^{-1}}{N} = \phi^{-1}(N) \tag{19}$$

Manipulating Eqs. (17), (18) and (19)

$$b(N) = -\delta\frac{R^{-1}}{N}\kappa + \delta\frac{R^{-1}}{N}E\big(\hat{\kappa}(N-1)\big) \tag{20}$$

From Eq. (20) we know that as $N \to \infty, b(N) = 0$ and $E[\hat{\kappa}(N)] = \kappa$.

Hence, the stabilized RLS converges asymptotically to the true value of the unknown parameter.

## Appendix B. Model used for post failure PID analysis

Nominal case:

$$\begin{bmatrix}\dot{\alpha}\\ \dot{q}\end{bmatrix}=\begin{bmatrix}-0.5341 & 0.9900\\ -7.7400 & -0.7173\end{bmatrix}\begin{bmatrix}\alpha\\ q\end{bmatrix}+\begin{bmatrix}-0.0280 & -0.0280\\ -5.7000 & -5.7000\end{bmatrix}\begin{bmatrix}\delta_{el}\\ \delta_{er}\end{bmatrix} \tag{21}$$

Failure case:

$$\begin{bmatrix}\dot{\alpha}\\ \dot{q}\end{bmatrix}=\begin{bmatrix}-0.5341 & 0.9900\\ -4.7200 & -0.3800\end{bmatrix}\begin{bmatrix}\alpha\\ q\end{bmatrix}+\begin{bmatrix}-9.4e-3 & -2.8e-2\\ -1.8990 & -5.700\end{bmatrix}\begin{bmatrix}\delta_{el}\\ \delta_{er}\end{bmatrix} \tag{22}$$

## Appendix C. Model used for stability margin estimation

$$\begin{bmatrix}\dot{\alpha}\\ \dot{q}\\ \dot{\theta}\\ \dot{u}/u_0\end{bmatrix}=\begin{bmatrix}-0.7771 & 1 & 0 & -0.1905\\ 0.3794 & -0.8329 & 0 & 0.0116\\ 0 & 1 & 0 & 0\\ -0.9371 & 0 & -0.0960 & -0.0296\end{bmatrix}\times\begin{bmatrix}\alpha\\ q\\ \theta\\ u/u_0\end{bmatrix}+\begin{bmatrix}-0.2960\\ -9.6952\\ 0\\ -0.0422\end{bmatrix}\delta_e \tag{23}$$

## References


[1] K. Basappa, R.V. Jategaonkar, Evaluation of recursive methods for aircraft parameter estimation, AIAA paper No. 2004-5063, USA.

[2] Yongsu Han, et al., Frequency and time domain online parameter estimation for reconfigurable flight control system, AIAA Paper No. 2009-2040, USA.

[3] Ravindra V. Jategaonkar, Flight Vehicle System Identification — A Time Domain Methodology, Progress in Astronautics and Aeronautics, vol. 216, AIAA, USA, 2006.

[4] C. Kamali, A.A. Pashilkar, J.R. Raol, Real time parameter estimation for reconfigurable control of unstable aircraft, Defense Science Journal 57 (4) (July 2007) 527–537.

[5] Vladislav Klein, Eugene A. Morelli, Aircraft System Identification: Theory and Practice, AIAA, USA, 2006.

[6] Eugene A. Morelli, Real-time parameter estimation in the frequency domain, in: AIAA Guidance, Navigation and Control Conference and Exhibit, USA, 1999, Paper No. AIAA-99-4043.

[7] Eugene A. Morelli, Practical aspects of the equation error method for aircraft parameter estimation, AIAA Paper No. 2006-6144, USA.

[8] Marcello R. Napolitano, Song Yongkyu, Brad Seanor, On-line parameter estimation for restructurable flight control systems, Aircraft Design 4 (2001) 19–50.

[9] Robert C. Nelson, Flight Stability and Automatic Control, Aerospace Series, McGraw–Hill International Editions, Singapore, 1990.

[10] Vijay V. Patel, Girish Deodhare, Shyam Chetty, Near real time stability margin estimation from piloted 3-2-1-1 inputs, in: AIAA Aircraft Technology Integration and Operations (ATIO2002), Technical Forum, October 2002.

[11] M.G. Perhinschi, et al., A simulation tool for on-line real time parameter estimation, AIAA Paper No. 2002-4685, USA.

[12] J.R. Raol, G. Girija, J. Singh, Modelling and Parameter Estimation of Dynamic Systems, IEE Control Engineering Book Series, vol. 65, IEE/IET, London, UK, 2004.

[13] D. Shore, M. Bodson, Flight testing of a reconfigurable control system on an unmanned aircraft, Journal of Guidance, Control and Dynamics 28 (4) (July–August 2005) 698–707.